THREE METHODS FOR EVALUATION OF FREQUENCY-DEPENDENT RESISTANCES AND INDUCTANCES OF MULTICONDUCTOR TRANSMISSION LINES

Antonije R. Djordjević
School of Electrical Engineering
University of Belgrade, Yugoslavia

Tapan K. Sarkar
Electrical and Computer Engineering Department
Syracuse University, Syracuse, N.Y. 13244-1240

Abstract. Three methods for the analysis of frequency-dependent resistances and inductances of multiconductor transmission lines are outlined and compared. The first method comes from power-engineering applications, and it is based on a numerical solution of an integral equation for the distribution of the conductor volume currents. The second method is based on the perturbation technique. The third method comes from high-frequency applications, and it is based on the principle of equivalent surface electric and magnetic currents.

1. INTRODUCTION

We consider a multiconductor transmission line, consisting of $(N+1)$ infinitely long cylindrical conductors of arbitrary cross sections (Figure 1). In the circuit-theory analysis of the response of such a line, usually the quasi-TEM approach is applied [Djordjević et al., 1987]. Thereby, one of the conductors is assumed to be the reference conductor ("ground"), for example conductor $\#(N+1)$, and the other N conductors are referred to as the signal conductors. In the circuit theory, the state of the line is represented in terms of currents of the signal conductors and voltages between the signal conductors and the reference conductor.

The circuit-theory analysis starts from the primary parameters of the line. For a multiconductor line, these parameters are the matrix $[B']$ of electrostatic-induction coefficients per unit length (often improperly referred to as the the capacitance matrix), the matrix $[G']$ of conductances per unit length, the matrix $[L']$ of inductances per unit length and the matrix $[R']$ of resistances per unit length. The dimensions of all these four matrices are N by N. Following the quasi-TEM approach, these matrices are evaluated from quasi-static analyses. More precisely, the matrices $[B']$ and $[G']$ are evaluated simultaneously from one electrostatic analysis of a two-dimensional system, in which the dielectric permittivity is taken to be complex [Djordjević et al., 1989]. The dielectric permittivities vary with frequency, and so do the matrices $[B']$ and $[G']$. In most practical cases, the relative variations of the matrix $[B']$ are very small, but they must be included in order to obtain a causal response in the time domain [Arabi et al., 1991].

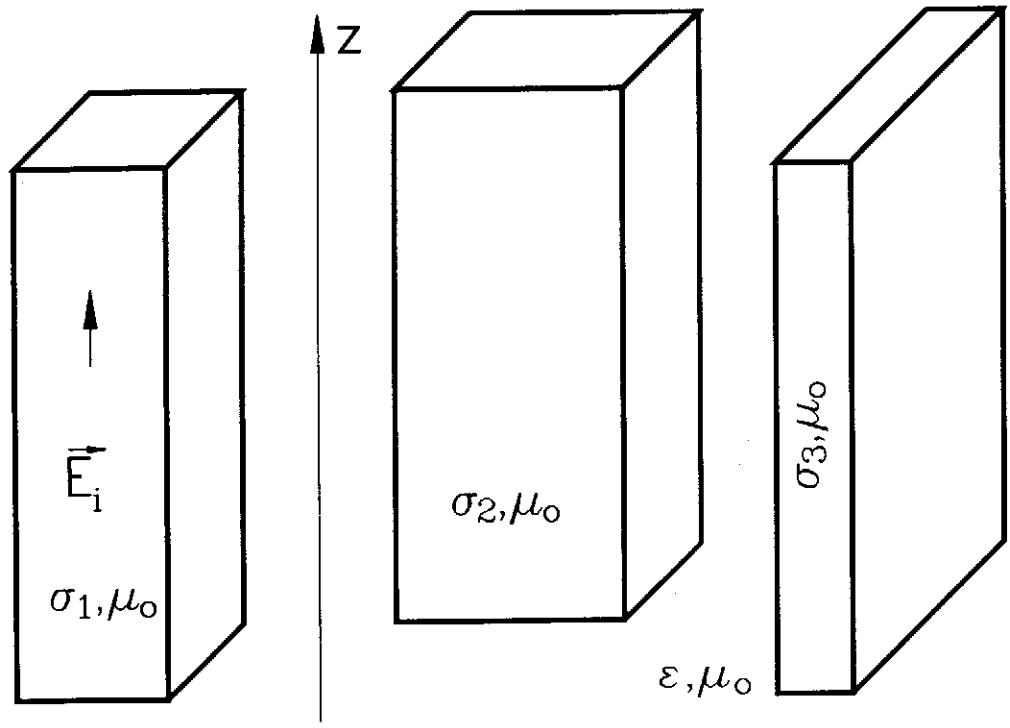

Figure 1. Sketch of a multiconductor transmission line (N=2).

The matrices $[L']$ and $[R']$ are evaluated from another analysis. In many cases, the results are required only for high frequencies, when the skin effect is fully developed. In those cases, the matrix $[L']$ is computed by inverting the matrix $[B'_o]$ which is evaluated when the transmission line dielectrics are replaced by vacuum, and the matrix $[R']$ is thereby evaluated by the perturbation method. The resulting matrix $[L']$ is frequency independent, while the matrix $[R']$ is proportional to $\sqrt{f}$, where f is the operating frequency. However, even in this case, a correction to the matrix $[L']$ is required in order to obtain a causal response, which consists in adding $[R']/\omega$ (where $\omega=2\pi f$ is the angular frequency) to the matrix $[L']$.

However, if a broader frequency range is of interest, the frequency variations of the matrices $[L']$ and $[R']$ are more complicated [Djordjević and Sarkar, 1994]. At the low-frequency end (towards the d.c. case), the current is practically uniformly distributed over a conductor cross section, there exist effects of the internal inductance, and the resistance tends to the d.c. value. In the intermediate region between the low and high frequencies, the edge and proximity effects take part in addition to the skin effect. These variations may be important not only for broadband signals in ordinary transmission lines, but also for integrated circuits, where the conductor thickness can be very small (e.g., thin-films), so that the skin effect need not be developed even in the gigahertz region.

The variations of the matrices $[L']$ and $[R']$ in a broad frequency range can be evaluated using several numerical techniques. We will concentrate our

attention to three of them. All of them treat the multiconductor transmission line of Figure 1 as a two-dimensional system, in which only axial currents are excited. For simplicity, we will assume the medium to be nonmagnetic everywhere.

The first technique is based on formulating an integral equation for the volume current distribution within the conductors, and it will be referred to as the volume-current method. This method has been successfully used for quite some time in solution of various power-engineering problems involving eddy currents [Popović and Popović, 1972]. The second method is a high-frequency approximation based on an electrostatic analysis with the perturbation technique [Djordjević et al., 1989], and it will be referred to as the perturbation method. The third method is a high-frequency technique, which is based on the equivalence theorems and the concept of equivalent surface currents, and it will be referred to as the surface-current method [Djordjević et al., 1985, Djordjević and Sarkar, 1986]. These three methods are briefly presented in Sections 2, 3 and 4, respectively, and in Section 5 a comparison between these techniques is given and illustrated by numerical examples. Thereby, the accuracy, ease of programming, cpu time and applicable frequency range of each method are evaluated. Of course, in addition to the three presented techniques there exist a variety of other methods for the analysis of multiconductor transmission lines which include the conductor losses [Faraji-Dana and Chow, 1990, Kiang, 1991]. The most sophisticated of these methods even take into account the dispersion effects of inhomogeneous dielectrics.

For all three techniques, each conductor of Figure 1 is assumed to be made of a linear homogeneous nonmagnetic material of a finite conductivity $(\sigma_1,\ldots,\sigma_{N+1})$. A time-harmonic regime is assumed, of an angular frequency ω. For each conductor the condition $\sigma \gg \omega\varepsilon_c$ is assumed to be fulfilled (where ε_c is the conductor permittivity), so that each conductor can be characterized by its complex permittivity $\varepsilon_e=-j\sigma/\omega$. The conductors are placed in a linear homogeneous dielectric, of parameters ε and μ_o. A Cartesian coordinate system is associated with the transmission line, where the z-axis is parallel to the conductor axis.

2. VOLUME-CURRENT METHOD

This technique has been applied in the solution of power-engineering problems of analyzing various buses [Popović and Popović, 1972]. It is based on formulating an integral equation for the distribution of the current within the conductor volume, and solving this equation using the method of moments [Harrington, 1993].

We assume that the excitation of the system of Figure 1 is modeled by an impressed (known) axial electric field ($\vec{E}_i=E_{iz}\hat{u}_z$, where $\hat{u}_z$ is the unit vector of the z-direction), which is uniform over the cross section of each conductor, as well as in the z-direction. This field actually replaces the axial component of the electric field produced by the transmission-line charges, as these charges are not included into the model [Djordjević et al.,

1985]. As a response to this field, axial volume currents are induced in the conductors. Their density ($\vec{J}=J_z\hat{u}_z$) depends only on the transverse coordinates, and not on z (two-dimensional case), and there are no charges associated with this current. At each point of a conductor, the current density is related to the electric field by

$$\vec{J} = \sigma(\vec{E} + \vec{E}_i) \ , \tag{1}$$

where $\vec{E}$ is the electric field produced by the conductor currents, and it can be expressed in terms of the magnetic vector-potential ($\vec{A}$) as

$$\vec{E} = -j\omega\vec{A} \ . \tag{2}$$

Assuming the medium to be nonmagnetic everywhere (i.e., $\mu=\mu_o$), and neglecting retardation in the dielectric in which the array of conductors is located (which is a valid assumption in power-engineering problems), the magnetic vector-potential is related to the currents, in the two-dimensional case, as

$$\vec{A} = -\frac{\mu_o}{2\pi}\int_S \vec{J}\,\log(r)\,dS \ , \tag{3}$$

where r is the distance between the source and the field points, and S denotes the cross section of all conductors, subject to the condition that the total current of the (N+1) conductors is zero,

$$\int_S \vec{J}\cdot d\vec{S} = 0 \ . \tag{4}$$

Equations (1-3) result in an integral equation for the z-component of the volume-current density vector (J_z),

$$-j\omega\frac{\mu_o}{2\pi}\int_S J_z(x',y')\,\log(r)\,dx'dy' + \frac{J_z(x,y)}{\sigma} = E_{iz}(x,y) \ , \tag{5}$$

which is valid for any point within any conductor of the line, where x and y are transverse coordinates. For convenience, the coordinates of the source point are denoted by primes, and

$$r = \sqrt{(x-x')^2+(y-y')^2} \ . \tag{6}$$

Equation (5) can be solved numerically, using the method of moments. The simplest choice is the pulse approximation for the current distribution. (More sophisticated approximations can involve entire-domain expansion functions, or even inclusion of skin-effect terms.) To that purpose, we divide the cross section of each conductor in a number of rectangular cells, and assume the current to be uniformly distributed over each cell. We utilize here equal-size cells, but a better policy would be to take cells to be progressively smaller going towards the conductor surfaces in order to obtain results valid in a broader frequency range [Dinh et al., 1990]. The simplest choice for testing is the point-matching method, with the matching points located at the cell centroids. The resulting integrals can be solved analytically. Having solved

for the current distribution, the total current of each conductor can be easily found.

The matrices $[R']$ and $[L']$ can be evaluated in the following way [Djordjević and Sarkar, 1986]. In order to properly model a TEM transmission line, the condition (4) must be fulfilled, which can be rewritten as

$$\sum_{m=1}^{N+1} I_m = 0 \ , \tag{7}$$

where the reference directions for conductor currents (I_m) coincide with the z-axis of Figure 1. The voltage drop per unit length between the signal conductor #m and the reference conductor is

$$\frac{dV_{m(N+1)}}{dz} = -(E_{imz} - E_{i(N+1)z}) \ . \tag{8}$$

From telegraphers' equations we have

$$\frac{d[V]}{dz} = -[Z'][I] = -([R']+j\omega[L'])\ [I] \ , \tag{9}$$

where $[V]$ is the vector of voltages between the signal conductors and the reference conductor, $[I]$ is the vector of signal conductor currents, and $[Z']$ is the matrix of line impedances per unit length. We introduce the augmented vector of currents of currents of all $(N+1)$ conductors, $[I^a]$, and the vector $[E_i]$ of impressed electric fields in the $(N+1)$ conductors. The system being linear, the following relation must be valid:

$$[I^a] = [T][E_i] \ , \tag{10}$$

where $[T]$ is a square matrix ($(N+1)$ by $(N+1)$). The matrix element T_{mn} numerically equals the current I_m when E_{inz}=1 V/m, and all the other impressed fields are zero. We now take n=1,...,$(N+1)$, solve equation (5) and hence evaluate the elements of the matrix $[T]$. Note that this procedure has no physical interpretation if the volume-current method is used, because each time the currents are evaluated, equation (4) is violated. Nevertheless, this numerical procedure yields correct final results for the matrices $[R']$ and $[L']$. From (10) we have

$$[E_i] = [Z^{a,}][I^a] \ , \tag{11}$$

where $[Z^{a,}] = [T]^{-1}$ is the augmented matrix of impedances per unit length. From equations (7-9) and (11) we can express the elements of the matrix $[Z']$ in terms of the elements of the matrix $[Z^{a,}]$ as

$$Z'_{mn} = Z^{a,}_{mn} - Z^{a,}_{m(N+1)} - Z^{a,}_{(N+1)n} + Z^{a,}_{(N+1)(N+1)} \ , \quad m,n=1,\ldots,N \ . \tag{12}$$

3. PERTURBATION METHOD

This is a well-known high-frequency approximation [Harrington, 1961], valid when the skin-effect is fully pronounced. In the analysis, the conductors are first assumed to be perfect, and the tangential magnetic field at the conductor surface ($\vec{H}_{tan}$) is evaluated. Then the conductors are assumed to have small losses, so that the magnetic field at the surface is negligibly affected by the presence of losses. The surface density of the power loss in the conductors is evaluated as

$$\frac{dP_c}{dS} = R_s |\vec{H}_{tan}|^2 , \tag{13}$$

where

$$R_s = \sqrt{\pi \mu_o f/\sigma} \tag{14}$$

is the surface resistance of the conductor. In the quasi-static analysis of transmission lines, the presence of inhomogeneous (nonmagnetic) dielectrics is assumed to have no influence on the distribution of the currents and magnetic field. Hence, the magnetic field is evaluated for the case when the dielectric is taken to be vacuum everywhere [Djordjević et al., 1989], which is reduced to solving a two-dimensional electrostatic problem. This solution is based on substituting the conductors by their surface free charges (of density ρ_s), located in vacuum. The current density can be expressed in terms of the charge density as $J=c_o\rho_s$, where $c_o=1/\sqrt{\varepsilon_o\mu_o}$. Setting the electric scalar-potential V at a conductor surface equal to the corresponding conductor potential, the following integral equation is obtained for the charge density

$$-\frac{1}{2\pi\varepsilon_o}\int_s \rho_s \log(r)\, ds = V , \tag{15}$$

where s denotes the contours of all conductors. Similarly to equation (3), equation (15) is valid only if the total charge of the system is zero, i.e.,

$$\int_s \rho_s\, ds = 0 . \tag{16}$$

The integral equation (16) is solved numerically, using the method of moments. The simplest approximation for the charge distribution are pulses (i.e., a piecewise-constant approximation), with the point-matching technique. The condition (16) can be forced if the last point-matching equation is subtracted from all the previous equations, and substituted by (16). The numerical accuracy is improved if the pulses are of nonuniform widths, being smaller in the regions where the charge density varies rapidly (such as near edges or wedges). Another improvement can be achieved by using Galerkin's technique [Harrington, 1993] instead of the point-matching. In any case, the resulting integrals can be evaluated explicitly, resulting in a very efficient technique for the analysis of arbitrary structures [Djordjević et al., 1989].

Having evaluated the conductor charge densities for a set of independent driving conditions, the matrix of electrostatic induction coefficients $[B'_o]$

can be calculated, and the external inductance matrix of the multiconductor transmission line is related to this matrix by

$$[L'_e] = \frac{1}{c_o^2} [B'_o]^{-1} . \tag{17}$$

The matrix $[R']$ is calculated from the power loss per unit length of the line, evaluated for various driving conditions of the line. From the boundary conditions for a perfect conductor, the density of the surface currents ($\vec{J}_s$) has the same magnitude as the intensity of the tangential magnetic field, so that the loss power per unit length of the transmission line is

$$P'_c = \int_s R_s J_s^2 \, dl . \tag{18}$$

The elements of the matrix $[R']$ are evaluated from the power P'_c when one signal conductor carries a current at a time, and when two signal conductors carry currents at a time, while the currents of other conductors is zero. The matrix [R'] varies with frequency as $\sqrt{f}$ due to equation (14). (In many practical cases, due to the surface roughness of the conductors, the measured conductor losses can be substantially higher than theoretically predicted for a smooth surface.) A more careful insight into the perturbation approach results in a reactive power in the conductors, in addition to the loss power (these two powers are equal in magnitude). This amounts to the internal inductance of the conductors which can be evaluated as

$$[L'_i] = [R']/\omega , \tag{19}$$

and which should be added to $[L'_e]$ to obtain $[L']$.

3. SURFACE-CURRENT METHOD

The basic idea of this method is to use equivalence theorems [Harrington, 1961] to break the system under considerations into a number of subsystems, each of them being filled with a homogeneous medium. To achieve this, a layer of surface electric currents (of density $\vec{J}_s$, which are in our case axial), and a layer of surface magnetic currents (of density $\vec{M}_s$, which are in our case transverse) must be placed on the conductor surfaces, with the objective to produce a zero total field in a region. The first subsystem consists of the region external to the conductors, with zero fields in the regions occupied by the conductors (external subsystem). The medium in the latter regions can be substituted by that of the external region, thus homogenizing the medium. The second subsystem (the first internal subsystem) consist of the internal region of the conductor #1, with zero field in the remaining space, which can be filled by the same medium of which conductor #1 is made, etc. [Djordjević et al., 1985]. For a transmission line of $(N+1)$ conductors, the number of internal subsystems is $(N+1)$. The homogenization of the medium is required in order to use a simple form of Green's functions in the equations for the potentials. For this technique we use retarded potentials, where Green's function for the two-dimensional case for the external subsystem is

$$g(r) = -\frac{j}{4} H_o^{(2)}(kr) \ , \tag{20}$$

where $H_o^{(2)}$ is Hankel's function of the second kind and order zero, and $k=\omega\sqrt{\varepsilon\mu}$. In the limiting quasi-static case Green's function (20) tends to $-\frac{1}{2\pi}\log(kr)$, thus yielding the kernels of equations (5) and (15). For an internal subsystem Green's function is

$$g(r) = \frac{1}{2\pi}\left[ker(|\gamma|r) + j\ kei(|\gamma|r)\right] \ , \tag{21}$$

where *ker* and *kei* are Kelvin's functions, and $\gamma=\sqrt{j\omega\mu\sigma}$ is the propagation coefficient in the conductor.

The fields can be expressed in terms of the potentials as

$$\vec{E} = -j\omega\vec{A} - \frac{1}{\varepsilon}\,\mathrm{curl}\,\vec{F} + \vec{E}_i \ , \tag{22}$$

$$\vec{H} = -j\omega\vec{F} - \mathrm{grad}\,V_m + \frac{1}{\mu}\,\mathrm{curl}\,\vec{A} + \vec{H}_i \ , \tag{23}$$

where $\vec{F}$ is the electric vector-potential, V_m the magnetic scalar-potential, and $\vec{E}_i$ and $\vec{H}_i$ impressed fields. (The -grad V term is missing in (22) because we again assume the electric currents to be z-directed, with no z-variation.) The potentials are given by

$$\vec{A} = \mu \int_s \vec{J}_s\, g(r)\, ds \ , \tag{24}$$

$$\vec{F} = \varepsilon \int_s \vec{M}_s\, g(r)\, ds \ , \tag{25}$$

$$V_m = \frac{1}{\mu}\int_s \rho_{ms}\, g(r)\, ds \ , \tag{26}$$

where

$$\rho_{ms} = \frac{j}{\omega}\,\mathrm{div}_s\,\vec{M}_s \tag{27}$$

is the density of surface magnetic charges. In our case $\mu=\mu_o$ everywhere.

In order to have a zero field within a region, we impose the boundary conditions that the tangential component of the electric field for the external subsystem is zero, i.e.,

$$\vec{E}_{tan} = 0 \ , \tag{28}$$

which leads to an electric-field integral equation (EFIE) for the equivalent surface currents. We also impose the boundary condition that the tangential

component of the magnetic field for each internal subsystem is zero, i.e.,

$$\vec{H}_{tan} = 0 \ , \tag{29}$$

which leads to magnetic-field integral equations (MFIE). As in the volume-current method, the impressed electric field, $\vec{E}_i$, is taken to be uniform over the cross section of each conductor, and this field replaces the field actually produces by the electric charges. This field is present only in the external subsystem. When the fields are expressed in terms of the potentials, and the potentials in terms of the equivalent surface sources, using equations (20-27), a set of coupled integral equations is obtained for $\vec{J}_s$ and $\vec{M}_s$.

An approximate solution of these equations is obtained using the simplest combination of pulse expansion functions and point-matching. Line magnetic charges are associated with this approximation of the magnetic currents. The pulses are taken to have nonuniform widths (narrower near wedges), and the matching points are located at the pulse midpoints, at the appropriate faces of the boundary surfaces (within regions occupied by conductors for the external subsystem, and outside the conductors for the internal subsystems). Taking into account

$$\text{grad } g(r) = \frac{dg}{dr} \hat{u}_r \ , \tag{30}$$

where $\hat{u}_r$ is the unit vector in the radial direction, for the external subsystem we have for the field components produced by an expansion function (carrying uniform surface currents of densities $\vec{J}_s$ and $\vec{M}_s$),

$$-j\omega\vec{A} = -j\zeta \vec{J}_s \int_s (-\tfrac{j}{4}) H_o^{(2)}(kr) \, d(ks) \ , \tag{31}$$

$$-\frac{1}{\varepsilon} \text{curl } \vec{F} = \vec{M}_s \times \int_s \frac{j}{4} H_o^{(2)}(kr) \hat{u}_r \, d(ks) \ , \tag{32}$$

where $\zeta=\sqrt{\mu/\varepsilon}$ is the wave impedance of the dielectric. For an internal subsystem we have similarly

$$-j\omega\vec{F} = -\frac{\vec{M}_s}{|\hat{\zeta}|} \int_s \frac{1}{2\pi} [ker(|\gamma|r) + j \, kei(|\gamma|r)] \, d(|\gamma|s) \ , \tag{33}$$

$$-\frac{1}{\varepsilon} \text{curl } \vec{A} = -\vec{J}_s \times \int_s \frac{1}{2\pi} [ker'(|\gamma|r) + j \, kei'(|\gamma|r)] \hat{u}_r \, d(|\gamma|s) \ , \tag{34}$$

$$-\text{grad } V_m = -|\vec{M}_s| \left[\frac{j}{2\pi|\hat{\zeta}|} [ker'(|\gamma|r) + j \, kei'(|\gamma|r) \hat{u}_r \right]_{r=r_1}^{r_2} \ , \tag{35}$$

where r_1 and r_2 are distances between the end points of a pulse and the field point, and $\hat{\zeta}=\sqrt{j\omega\mu/\sigma}$ is the wave conductor impedance.

The above system is solved for a set of independent driving conditions, following a similar procedure as for the volume-current method. Hereby, the current of a conductor is obtained by integrating the surface-current density $\vec{J}_s$ around the conductor circumference. The matrices $[R']$ and $[L']$ can now be evaluated from equations (9-12).

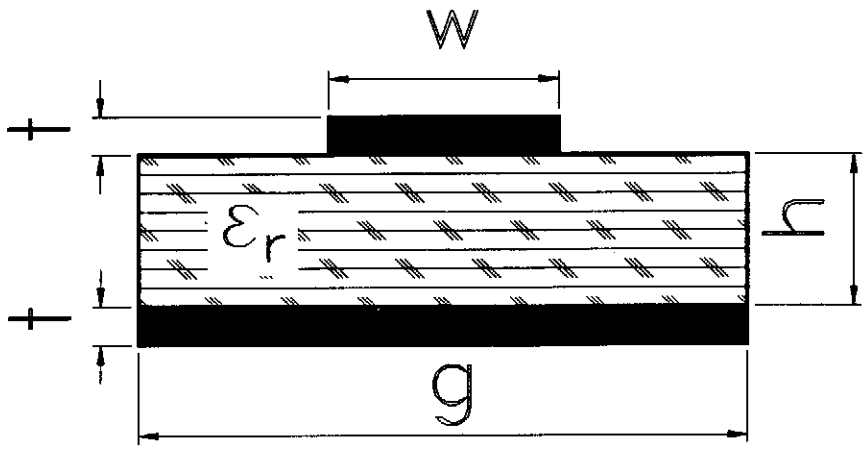

Figure 2. Sketch of a microstrip line.

5. EXAMPLES

The first example is the microstrip line, sketched in Figure 2, of dimensions w=0.2 mm, h=0.1 mm, g=2 mm, and t=0.01 mm. The conductors are made of copper, of conductivity σ=56 MS/m. Shown in Table 1 are the resistance per unit length and the inductance per unit length of this line, versus frequency, obtained by the three techniques presented in this paper. For the volume-current method, the conductors were uniformly divided into pulses (rectangles): n_w=10 along w, n_g=40 along g and n_t=3 along t, resulting in the total of 150 unknowns. For the perturbation technique, the numbers of nonuniformly distributed pulses were n_w=25, n_t=3 and n_g=85 along the corresponding lengths, resulting in a total of 141 unknowns (the thickness of the ground plane was taken to be zero). For the surface-current method, the number of nonuniformly distributed pulses were n_w=25, n_g=50 and n_t=3, respectively, resulting in a total of 324 unknowns (for electric and magnetic currents).

Table 1 illustrates some features of the three techniques. The volume-current method yields excellent results at low frequencies. For example, for f=10 kHz, the numerical results are L'=440.5 nH/m and R'=9.821 Ω/m, while the analytically calculated values [Djordjević and Sarkar, 1993] are L'=439.27 nH/m and R'=9.821 Ω/m. The surface-current method yields a smaller accuracy, especially as the frequency becomes very low. The accuracy can be improved at the expense of taking more pulses. The results of the perturbation method for low frequencies are a large underestimate of R' and an overestimate of L', and they are practically useless.

In the medium-frequency region (300 kHz-50 MHz) the agreement between the volume-current and surface-current methods is excellent, while the results of the perturbation method are still poor. Above about 100 MHz, in the high-frequency (skin-effect) region, the results for R' obtained by the volume-current method tend to saturate, instead of increasing as $\sqrt{f}$. This is due to the pulse approximation for the current distribution, as there must always be a current in the outermost layer of pulses. In the real system, however, the thickness of the current layer constantly decreases with increasing the frequency. The results for R' obtained by the surface-current method follow very well the $\sqrt{f}$ behavior and they are facein a good agreement with the perturbation method. However, at very high frequencies (above about 10 GHz) R' obtained by the surface-current method starts increasing much faster. This is a consequence of radiation. Namely, the structure behaves like a two-dimensional magnetic dipole, the radiation resistance of which is proportional to f^3 [Djordjević et al., 1985]. There would be no radiation effects in the numerical model if the quasi-static kernel of equation (5) were used instead of (20).

Table 1. Primary parameters of microstrip line sketched in Figure 2.

f [Hz]	Volume-current method		Perturbation method		Surface-current method	
	R' [Ω/m]	L' [nH/m]	R' [Ω/m]	L' [nH/m]	R' [Ω/m]	L' [nH/m]
10.00 k	9.821	440.5	0.131	2365.	9.630	431.9
17.78 k	9.822	440.5	0.174	1845.	9.630	433.1
31.62 k	9.822	440.5	0.232	1456.	9.630	434.2
56.23 k	9.823	440.4	0.310	1163.0	9.631	435.3
100.0 k	9.826	440.2	0.413	943.8	9.633	436.1
177.8 k	9.835	439.3	0.551	779.3	9.642	436.2
316.2 k	9.862	436.7	0.735	656.0	9.669	434.4
562.3 k	9.942	429.3	0.980	563.6	9.749	427.4
1.000 M	10.14	411.6	1.306	494.2	9.946	409.6
1.778 M	10.48	382.5	1.742	442.2	10.29	380.2
3.162 M	10.87	353.3	2.323	403.2	10.68	350.6
5.623 M	11.23	333.7	3.098	374.0	11.05	330.9
10.00 M	11.59	322.9	4.131	352.0	11.43	320.2
17.78 M	12.07	316.3	5.509	335.6	11.94	313.6
31.62 M	12.67	311.8	7.346	333.3	12.69	308.8
56.23 M	13.40	308.7	9.796	314.0	13.80	305.1
100.0 M	14.42	306.7	13.06	307.1	15.61	302.4
177.8 M	16.13	305.1	17.42	301.9	18.70	299.7
316.2 M	18.72	303.5	23.23	298.0	23.54	297.2
562.3 M	22.14	302.3	30.98	295.1	30.80	294.9
1.000 G	26.42	301.3	41.31	292.9	41.54	293.0
1.778 G	30.27	300.5	55.09	291.2	55.64	291.3
3.162 G	32.38	300.1	73.46	290.0	73.73	290.1
5.623 G	33.24	300.0	97.96	289.1	98.1	289.3
10.00 G	33.52	299.9	130.6	288.4	133.7	288.7
17.78 G	33.61	299.9	174.2	287.9	199.2	288.7
31.62 G	33.64	299.9	232.3	287.5	387.5	289.5

The second example are two coupled microstrip lines, sketched in Figure 3, of dimensions w=0.6 mm, s=0.02 mm, g=2 mm, h=0.1 mm, t=0.02 mm, and the

conductors are made of copper. Given in Table 2 are the elements of the matrices $[R']$ and $[L']$ for several frequencies, as computed by the three techniques. For comparison, the exact d.c. values for the elements of the matrix $[R']$ are $R'_{11}=R'_{22}=1.935$ Ω/m and $R'_{12}=R'_{21}=0.446$ Ω/m. This example confirms the conclusions drawn from the previous example about the behavior of the results of the three methods.

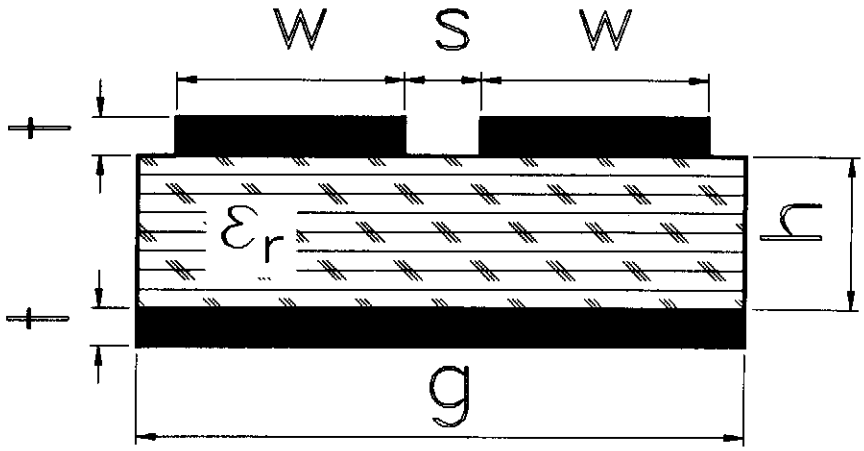

Figure 3. Sketch of two coupled microstrip lines.

Table 2. Primary parameters of coupled microstrip lines sketched in Figure 3.

f [Hz]	Volume-current mehod		Perturbation mehod		Surface-current mehod	
	$R'_{11}=R'_{22}$ $R'_{12}=R'_{21}$ [Ω/m]	$L'_{11}=L'_{22}$ $L'_{12}=L'_{21}$ [nH/m]	$R'_{11}=R'_{22}$ $R'_{12}=R'_{21}$ [Ω/m]	$L'_{11}=L'_{22}$ $L'_{12}=L'_{21}$ [nH/m]	$R'_{11}=R'_{22}$ $R'_{12}=R'_{21}$ [Ω/m]	$L'_{11}=L'_{22}$ $L'_{12}=L'_{21}$ [nH/m]
10.00 k	1.935 0.446	253.9 -26.4	0.074 -0.008	1309. -90.7	1.898 0.459	247.8 -24.3
100.0 k	1.945 0.440	250.7 -23.9	0.235 -0.025	501.7 -3.7	1.908 0.451	247.9 -23.1
1.000 M	2.183 0.316	187.1 15.6	0.742 -0.080	246.3 23.9	2.149 0.327	184.8 16.5
10.00 M	2.576 0.161	156.2 30.2	2.347 -0.253	165.6 32.6	2.694 0.075	152.8 11.9
100.0 M	4.653 0.912	149.1 29.9	7.422 -0.800	140.0 35.3	6.829 -0.263	139.7 35.4
1.000 G	7.576 1.437	146.0 29.0	23.47 -2.53	131.9 36.2	23.28 -2.25	131.9 36.1
10.00 G	7.748 1.457	145.9 29.0	74.22 -8.00	129.4 36.5	77.19 -1.80	122.9 36.4

Regarding the complexity of the programing, the volume-current method is simplest, the perturbation method is somewhat more complicated, and the surface-current method is much more complicated than the other two methods. Regarding the c.p.u. time, the perturbation technique is faster than the other

two methods even if only one frequency is considered, because for a given accuracy (in the high-frequency region, where this method is valid) it usually requires much less unknowns than the other two methods, and it involves only real arithmetics. In addition, results for various frequencies can thereafter be obtained even by hand calculations. The c.p.u. times of the volume-current and surface-current methods are comparable in most cases.

6. CONCLUSION

Three numerical methods for analysis the frequency-dependent matrices of resistances and inductances per unit length of multiconductor transmission lines are presented and compared. The overall performance of the volume-current method is best at low and medium frequencies (when the skin effect is not yet developed), but it can be extended into the skin effect region using nonuniform segmentation, adapted to the skin depth at the highest operating frequency. For the frequencies deep in the skin-effect region, the perturbation technique is superior. The surface-current method is the only one that covers the full frequency range, at the expense of a more complex programing than the other two techniques, and a somewhat reduced accuracy at very low frequencies. Therefore, a combination of the volume-current method and the perturbation method seems to be the best choice for most applications, with a particular caution taken to obtain a good overlap of results at the beginning of the high-frequency region (when the skin depth is of the order of the conductor thickness). However, the surface-current method is indispensable for an independent check of the results in this transition region.

REFERENCES

Arabi, T.R., Murphy, A.T., Sarkar, T.K., Harrington, R.F., Djordjević, A.R., "On the modeling of conductor and substrate losses in multiconductor, multidielectric transmission line systems", *IEEE Trans. on Microwave Theory and Techniques*, vol. MTT-39, no. 7, pp. 1090-1097, July 1981.

Dinh, T. Vu, Cabon, B., Chilo, J., "Time domain analysis of skin effect on lossy interconnections", *Electronics Letters*, vol. 26, no. 25., pp. 2057-2058, December 1990.

Djordjević, A.R., Sarkar, T.K., Rao, S.M., "Analysis of finite conductivity cylindrical conductors excited by axially-independent TM electromagnetic field", *IEEE Trans. on Microwave Theory and Techniques*, vol. MTT-33, no. 10, pp. 960-966, October 1985.

Djordjević, A.R., Sarkar, T.K., "Frequency behaviour of multiconductor transmission line inductances and resistances", *Archiv für Elektronik und Übertragungstechnik*, B. 40, H. 4, pp.254-256, April 1986.

Djordjević, A.R., Sarkar, T.K., Harrington, R.F., "Time-domain response of multiconductor transmission lines", *Proc. IEEE*, vol.75, no. 6, pp. 743-764, June 1987.

Djordjević, A.R., Harrington, R.F., Sarkar, T.K., Bažđar, M.B., *Matrix Parameters for Multiconductor Transmission Lines (Software and User's Manual)*, Boston: Artech House, 1989.

Djordjević, A.R., Sarkar, T.K., "Closed-form formulas for frequency-dependent

resistance and inductance per unit length of microstrip and strip transmission lines", in print in *IEEE Trans. on Microwave Theory and Techniques*, 1994.

Faraji-Dana,R., Chow,Y. L., "The current distribution and AC resistance of a microstrip structure", *IEEE Trans. on Microwave Theory and Techniques*, vol. 38, no. 9, pp. 1268-1277, September 1990.

Harrington,R.F., *Time-Harmonic Electromagnetic Fields*, New York: McGraw-Hill, 1961.

Harrington,R.F., *Field Computation by Moment Methods*, New York: IEEE Press, 1993.

Kiang,J.F., "Integral equation solution to the skin effect problem on conductor strips of finite thickness", *IEEE Trans. on Microwave Theory and Techniques*, vol. 39, no. 3, pp. 452-460, March 1991.

Popović,B.D., Popović,Z.D., "Method for determining power-frequency current distribution in cylindrical conductors", *Proc. IEE*, vol. 119, no.5, pp. 569-574, May 1972.